

Detection of supernovae neutrinos with neutrino-iron scattering

A.R. Samana and C.A. Bertulani

*Department of Physics, Texas A&M University Commerce,
P.O.3011 Commerce, 75429 TX, USA*

(Dated: July 28, 2008)

The $\nu_e - {}^{56}\text{Fe}$ cross section is evaluated in the projected quasiparticle random phase approximation (PQRPA). This model solves the puzzle observed in RPA for nuclei with mass around ${}^{12}\text{C}$, because it is the only RPA model that treats the Pauli principle correctly. The cross sections as a function of the incident neutrino energy are compared with recent theoretical calculations of similar models. The average cross section weighted with the flux spectrum yields a good agreement with the experimental data. The expected number of events in the detection of supernova neutrinos is calculated for the LVD detector leading to an upper limit for the electron neutrino energy of particular importance in this experiment.

PACS numbers: 23.40.-s, 25.30.Pt, 26.50.+x

A careful knowledge of the semileptonic weak interactions in nuclei allows the possibility of testing implications of physics beyond the standard model, such as exotic properties of neutrino oscillations and massiveness. The dynamics of supernova collapse and explosions as well as the synthesis of heavy nuclei are strongly dominated by neutrinos. For example, neutrinos carry away about 99% of gravitational binding energy in the core-collapse of a massive star, and only a small fraction ($\sim 1\%$) is transferred to the stalled shock front, creating ejected neutrino fluxes observed in supernova remnants [1].

It was shown in Ref. [2] that accurate nuclear structure calculations are essential to constrain the neutrino oscillations parameters of the LSND experiment [3]. This was also noted in previous works, e.g. Hayes *et al.* in Ref. [4]. In that work, based on a shell model, the same exclusive cross section in ${}^{12}\text{C}$ is obtained as with another shell model used in Ref [5]. This shows the importance of including configuration mixing (as done in both references) for this nucleus [37]. Nevertheless the QRPA predictions of Ref. [5] do not yield good results for this nucleus because the configuration mixing is not properly accounted for and the projection procedure (as done in Ref. [7]) is not included. In particular, the employment of PQRPA for the inclusive ${}^{12}\text{C}(\nu_e, e^-){}^{12}\text{N}$ cross section, instead of the continuum RPA (CRPA) used by the LSND collaboration in the analysis of $\nu_\mu \rightarrow \nu_e$ oscillations of the 1993-1995 data sample, leads to an increased oscillation probability. Then, the previously found consistency between the $(\sin^2 2\theta, \Delta m^2)$ confidence level regions for the $\nu_\mu \rightarrow \nu_e$ and the $\bar{\nu}_\mu \rightarrow \bar{\nu}_e$ oscillations is decreased [2].

The measured observables are flux-averaged cross sections. The KARMEN Collaboration measured charged and neutral cross sections induced on ${}^{12}\text{C}$ [8]. They also measured (the only experimental data for a medium-heavy nucleus) the neutrino reaction ${}^{56}\text{Fe}(\nu_e, e^-){}^{56}\text{Co}$ from e^- -bremsstrahlung with the detector surrounding shield [9]. This cross section is important to test the ability of nuclear models in explaining reactions on nuclei with masses around iron, which play an important

role in supernova collapse [10]. Experiments on neutrino oscillations such as MINOS [11] use iron as material detector, and future experiments, such as SNS at ORNL [12] plan to use the same material.

In a recent work, Agafonova *et al.* [13] studied the effect of neutrino oscillations on the supernova neutrino signal with the LVD detector. This detector studies supernova neutrinos through their interactions with protons and carbon nuclei in a liquid scintillator and with iron nuclei in the support structure. Several estimates on deviations of the detected signal arising from different constraints on the astrophysical parameters, oscillation parameters and the non-thermal nature of the neutrino fluxes were studied before [13]. Nevertheless, in all their estimates the corresponding ν -nucleus cross sections were kept within strict limits.

In this work, we calculate the $\nu_e - {}^{56}\text{Fe}$ cross sections using QRPA and PQRPA models to account for allowed and forbidden transitions. The present calculations are the first within the PQRPA framework for this purpose. In Ref. [14] it was established that PQRPA is the proper theory to treat both short range pairing and long range random-phase (RPA) correlations. When QRPA was implemented for the triad $\{{}^{12}\text{B}, {}^{12}\text{C}, {}^{12}\text{N}\}$ there were difficulties in choosing the ground state of ${}^{12}\text{N}$ because the lowest state is not the most collective [5]. PQRPA solves this puzzle because it treats correctly the Pauli Principle, yielding better results for the distribution of the Gamow-Teller (GT) strength. This problem does not exist in heavier nuclei, where the neutron excess allows QRPA to account for pairing and RPA correlations [15]. In the case of medium-heavy nuclei, such as ${}^{56}\text{Fe}$, the consequences of the projection technique procedure can be manifest.

Many calculations of the ${}^{56}\text{Fe}(\nu_e, e^-){}^{56}\text{Co}$ cross sections with microscopic and global models have been reported previously. The first were shell model calculations developed by Bugaev *et al.* [16]. They obtained the ν -nucleus cross sections as a function of the incident neutrino energy. A second estimate was obtained by Kolbe *et al.* [17] using a nuclear Hybrid model: shell model for the GT and Fermi (F) transitions, and continuum RPA

(CRPA) for forbidden transitions. This cross section was employed to estimate the number of events from ν - ^{56}Fe reactions in the LVD detector [13]. Lazauskas *et al.* [18] used QRPA with the Skyrme force to explore the possibility of performing nuclear structure studies using neutrinos from low energy beta-beams [19]. Several ν -nucleus cross sections for different nuclei were also obtained recently with the relativistic QRPA (RQRPA) [20]. The ν - ^{56}Fe cross sections were also described with the gross theory of beta decay (GTBD) [21].

The cross section for $\nu_e + (Z, A) \rightarrow (Z + 1, A) + e^-$ is given by

$$\sigma(E_e, J_f) = \frac{|\mathbf{p}_e|E_e}{2\pi} F(Z + 1, E_e) \int_{-1}^1 d(\cos \theta) \mathcal{T}_\sigma(|\mathbf{k}|, J_f), \quad (1)$$

where $F(Z + 1, E_e)$ is the usual scattering Fermi function, $k = p_e - q_\nu$ is the momentum transfer, p_e and q_ν are the corresponding electron and neutrino momenta, and $\theta \equiv \hat{\mathbf{q}}_\nu \cdot \hat{\mathbf{p}}_e$ is the angle between the incident neutrino and emerging electron. The $\sigma(E_e, J_f)$ cross section is obtained within first-order perturbation theory according to Ref. [7], where velocity-dependent terms are included in the weak effective Hamiltonian. The transition amplitude $\mathcal{T}_\sigma(|\mathbf{k}|, J_f)$ depends on the neutrino leptonic traces and on the nuclear matrix elements (NME), as explained in Ref. [7]. Here, the NME are evaluated in QRPA and in PQRPA. We employ the δ -interaction (in MeV fm^3)

$$V = -4\pi (v_s P_s + v_t P_t) \delta(r),$$

with different coupling constants v_s and v_t for the particle-hole, particle-particle, and pairing channels. This interaction was used in Refs. [22, 23, 24, 25] leading to a good description of single and double β -decays.

For ^{56}Fe we work within a configuration space of 12 single-particle levels, including the oscillator shells $2\hbar\omega$, $3\hbar\omega$ and $4\hbar\omega$. The single-particle energies of the active $3\hbar\omega$ shell correspond to the experimental energies of ^{56}Ni . For the other $2\hbar\omega$ and $4\hbar\omega$ shells we have used the harmonic oscillator energies with $\hbar\omega/\text{MeV} = 45 A^{1/3} - 25 A^{2/3}$. The parameters $v_s^{pair}(p)$ and $v_s^{pair}(n)$ were obtained with the procedure of Ref. [26], *i.e.*, by fitting the experimental gap pairing energies of protons and neutrons, $\Delta_{n,p}(N, Z)$ (eq.(2.96) of Ref. [27]), to $\Delta_{n,p}$ defined by the usual BCS equations. The BCS or PBCS equations were solved in the full space of three oscillator shells. For the particle-hole channel we have used $v_s^{ph} = 27$ and $v_t^{ph} = 64$ (in MeV fm^3). These values were fitted to ^{48}Ca from a systematic study of the GT resonances [25] and shown to yield a good description of double beta decay. For the particle-particle channel, it is convenient to define the parameters

$$s = \frac{2v_s^{pp}}{v_s^{pair}(p) + v_s^{pair}(n)},$$

and

$$t = \frac{2v_t^{pp}}{v_s^{pair}(p) + v_s^{pair}(n)},$$

associated to the coupling constant of the $T = 1, S = 0$ (singlet) and $T = 0, S = 1$ (triplet) channels respectively Ref. [25]. We adopt $s \simeq 1$, which restores the isospin symmetry in QRPA for $N > Z$. As the experimental errors in the averaged cross sections are very large, the agreement of the theoretical cross section is not sufficient to select the best nuclear structure calculation and other observables must be found. We use the behavior of the $B(GT^-)$ strength as function of the parameter t to conclude that better results could be obtained when the particle-particle channel is off, $t = 0$. With this value the theoretical value ($B(GT^-) = 17.7$) overestimates the experimental value (9.9 ± 2.4 [29]) similarly to previous and more sophisticated QRPA calculations for ^{56}Fe ($B(GT^-) = 18.68$ [30]) with the Skyrme force.

The flux averaged inclusive cross section reads

$$\langle \sigma_e \rangle = \int dE_\nu \sigma(E_\nu) n(E_\nu), \quad (2)$$

where $\sigma_e(E_\nu) = \sum_{J_f^\pi} \sigma_e(E_e, J_f^\pi)$, is the inclusive cross section as a function of the neutrino energy and $n(E_\nu)$ is the neutrino normalized flux. As a first test, we fold the $\sigma_e(E_\nu)$ with the Michel energy spectrum [17],

$$n(E_\nu) = \frac{96E_\nu^2}{M_\mu^4} (M_\mu - 2E_\nu), \quad (3)$$

where M_μ is the muon mass. In Table I we compare our $^{56}\text{Fe}(\nu_e, e^-)^{56}\text{Co}$ cross section $\langle \sigma_e \rangle$ in QRPA and PQRPA with other nuclear models for the energy window of μ -Decay-At-Rest (DAR) neutrinos that the KARMEN experiment observed.

TABLE I: Comparison of $\langle \sigma_e \rangle$ in 10^{-42} cm^2 for $^{56}\text{Fe}(\nu_e, e^-)^{56}\text{Co}$ obtained in our QRPA and PQRPA confronted with other nuclear models. For the Hybrid model [17] we denote with (a) partial occupation in the ground state and with (b) no occupation.

Model	$\langle \sigma_e \rangle$
QRPA	264.6
PQRPA	197.3
Hybrid ^(a) [17]	228.9
Hybrid ^(b) [17]	238.1
TM [31]	214
RPA [32]	277
QRPA _s [18]	352
RQRPA [20]	140
Exp[9]	$256 \pm 108 \pm 43$

From Table I we note that our results for $\langle \sigma_e \rangle = 264.6 \times 10^{-42} \text{ cm}^2$ (QRPA), and $197.3 \times 10^{-42} \text{ cm}^2$ (PQRPA) are

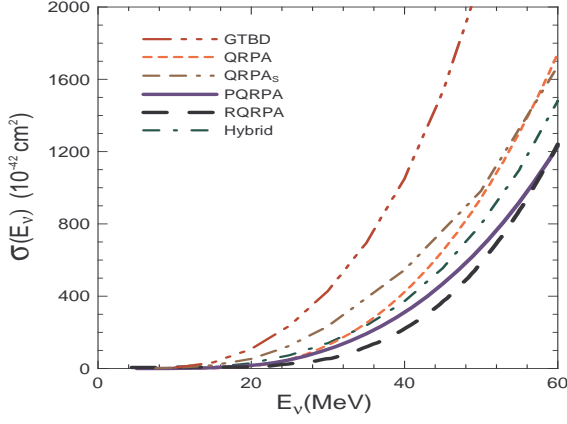


FIG. 1: (Color online) Inclusive $^{56}\text{Fe}(\nu_e, e^-)^{56}\text{Co}$ cross sections (in 10^{-42} cm^2) evaluated in QRPA (dashed line) and PQRPA (solid line), in the DAR region, are compared with those obtained with other nuclear structure models: GTBD (dashed-dot-dot-dot line) [21], Hybrid (dashed-dot line) [28], QRPA_s (dashed-dot dot line) [18], and RQRPA (dashed line) [20].

in agreement with the experimental value $256 \pm 83(\text{stat}) \pm 42(\text{syst}) \times 10^{-42} \text{ cm}^2$ [9]. The main difference between QRPA and PQRPA, both solved consistently with the same interaction, shows that the projection procedure is important in a medium mass nucleus such as ^{56}Fe .

In Figure 1 we plot the inclusive $^{56}\text{Fe}(\nu_e, e^-)^{56}\text{Co}$ cross sections (in 10^{-42} cm^2) evaluated in QRPA (dashed line) and PQRPA (solid line), in the DAR region. A comparison is shown with other nuclear structure models. All models yield the same energy dependence that goes approximately as E_ν^2 for low incident neutrino energies, except for the GTBD model, which shows a large deviation from the other cross sections.

Figure 2 excludes the GTBD results and extends the energy scale to 100 MeV (supernova neutrino energies). $\sigma(E_\nu)$ reaches the DAR energy region at $E_\nu \sim 60 \text{ MeV}$. Beyond that the QRPA result is above the other models. Nevertheless, the PQRPA cross section lies below, showing the effect of the projection procedure. In this region, the main contribution arises from the non-allowed transitions, as found in previous works [18, 20].

The number of events detected for supernova explosions is calculated as,

$$N_\alpha = N_t \int_0^\infty \mathcal{F}_\alpha(E_\nu) \cdot \sigma(E_\nu) \cdot \epsilon(E_\nu) dE_\nu, \quad (4)$$

where the index $\alpha = \nu_e, \bar{\nu}_e, \nu_x$ and ($\nu_x = \nu_\tau, \nu_\mu, \bar{\nu}_\mu, \bar{\nu}_\tau$) indicates the neutrino or antineutrino type, N_t is the number of target nuclei, $\mathcal{F}_\alpha(E_\nu)$ is the neutrino flux, $\sigma(E_\nu)$ is the neutrino-nucleus cross section, $\epsilon(E_\nu)$ is the detection efficiency, and E_ν is the neutrino energy. Recent calculations by the LVD group [13] estimate that the $(\nu_e + \bar{\nu}_e)$ interactions on ^{56}Fe are almost 17% of the total detected signal.

The time-spectra can be approximated by the zero-pinch Fermi-Dirac distribution. For the neutrino of

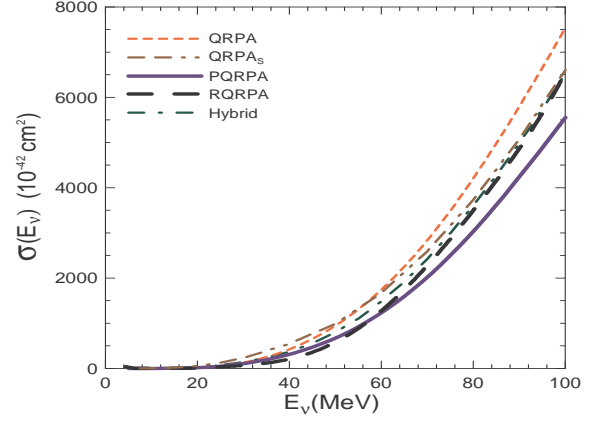


FIG. 2: (Color online) Same as in Figure 1. The inclusive cross sections (in 10^{-42} cm^2) are shown. In this case, the neutrino energy window is characteristic of the LVD experiment.

flavor α , it is

$$\mathcal{F}_\alpha^0(E_\nu, T_{\nu_\alpha}) = \frac{L_\alpha}{4\pi D^2 T_\alpha^4 F_3(0)} \frac{E_\nu^2}{\exp(E_\nu/T_\alpha) + 1}, \quad (5)$$

where D is the distance to the supernova, E_ν is the neutrino energy, L_α is the time-integrated energy of flavor ν_α , T_α is the neutrino effective temperature, and $F_3(0) \equiv \int_0^\infty d^3x x^3/(e^x + 1)$ is the normalization factor. For a galactic supernova explosion at a typical distance $D = 10 \text{ kpc}$, it was assumed that the total binding energy for each flavor is $L_\alpha = f_{\nu_\alpha} E_b$, with $E_b = 3 \times 10^{53} \text{ erg}$, and a perfect energy equipartition between the neutrino flavors, $f_\alpha = f_{\nu_e} = f_{\bar{\nu}_e} = f_{\nu_x} = 1/6$. Hence, it is possible to assume that the fluxes $(\nu_\mu, \nu_\tau, \bar{\nu}_\mu, \bar{\nu}_\tau)$ are identical. Because the pinched factor was assumed zero for all neutrino flavors, we can fix the effective neutrino temperature as $T_{\nu_x} = 1.5T_{\bar{\nu}_e}$ and $T_{\nu_e} = 0.8T_{\bar{\nu}_e}$, leaving $T_{\bar{\nu}_e}$ as a variable parameter in the interval studied in Ref. [13].

When the neutrinos escape from the star, they cross regions of different densities where a flavor transition could happen. Usually one assumes two resonance layers which we call Mikheyev-Smirnov-Wolfenstein (MSW) resonances throughout the text (see for example Ref. [33]). According to the mass scheme shown in [13], the observed electron neutrino fluxes ($\mathcal{F}_{\nu_e}, \mathcal{F}_{\bar{\nu}_e}$) originating from MSW resonances are linear combinations of the original neutrinos fluxes in the star, $\mathcal{F}_{\nu_e}^0$ and $\mathcal{F}_{\nu_x}^0$, with coefficients governed by the crossing probability in the high density resonance layer, $P_H(\Delta_{atm}^2, \theta_{13})$. For simplicity, we only show differences that appear in the number of events calculated from the convolution of cross sections obtained with different nuclear structure models with the original supernova fluxes, *i.e.*,

$$N_e \equiv N_e(T_{\nu_e}) = N_t \int_0^\infty \mathcal{F}_e^0(E_\nu, T_{\nu_e}) \cdot \sigma_e(E_\nu) \cdot \epsilon(E_\nu) dE_\nu, \quad (6)$$

for “direct” electron neutrino event, and

$$\tilde{N}_e \equiv \tilde{N}_e(T_{\nu_x}) = N_t \int_0^\infty \mathcal{F}_x^0(E_\nu, T_{\nu_x}) \cdot \sigma_e(E_\nu) \cdot \epsilon(E_\nu) dE_\nu, \quad (7)$$

for the “indirect” number of events for electron neutrino associated to the total ν_e -flux coming from the contribution of \mathcal{F}_x^0 . Due to the MSW effect, electron neutrino fluxes mix with non-electron neutrino fluxes (*i.e.*, $\nu_x \equiv \nu_\mu, \nu_\tau$), and therefore with the MSW resonance the ν_e ’s might get a “hot” contribution to their flux. Another important issue, not considered for simplicity in the present work, is the spectral swapping of the neutrino flux (Ref. [34]). Duan *et al.* have shown that certain numerical results in the simulation of neutrino and antineutrino flavor evolution in the region above the post-supernova explosion proto-neutron star cannot be easily explained with the conventional MSW mechanism Ref. [1].

For the neutrino reactions $^{56}\text{Fe}(\nu_e, e^-)^{56}\text{Co}$, we calculate N_e and \tilde{N}_e as a function of the neutrino temperatures T_{ν_e} and T_{ν_x} , folding $\sigma_e(E_\nu)$ from different nuclear structure models with the neutrino fluxes $\mathcal{F}_{\nu_e}^0(E_\nu, T_{\nu_e})$ and $\mathcal{F}_{\nu_x}^0(E_\nu, T_{\nu_x})$, respectively. The limits for the temperatures, T_{ν_e} and T_{ν_x} , were obtained from the interval $T_{\nu_e} \in [4, 7]$ MeV and the relations $T_{\nu_x} = 1.5T_{\nu_e}$ and $T_{\nu_e} = 0.8T_{\nu_x}$, employed by the LVD group [13]. The $\epsilon(E_\nu)$ efficiency is taken from Figure 1b of Ref. [13]. The results obtained are shown in Figure 3. The left panel shows the number of events for electron neutrinos, N_e , with different $\sigma_e(E_\nu)$, our QRPA and PQRPA, QRPA_s [18], RQRPA [20] and the Hybrid model [17] employed by the LVD detector. On the right panel we show the number of events \tilde{N}_e . Although one knows that ν_x neutrinos at supernova energies can only induce neutral current events, we evaluate this quantity because it will be modified by MSW oscillations according to the scheme presented in equations (2) and (4) of Ref. [13], or in equations (10) and (12) of Ref. [35]. Despite it is certain that the \tilde{N}_e could be obtained from the expression for N_e extending the interval of T_{ν_e} to cover the interval T_{ν_x} , this region ($T_{\nu_e} \in [6, 10.5]$ MeV) of temperature for ν_e is not in agreement with the physical range depending on the neutrino transport that it is predicted by different supernova modelers, as such in Ref. [36].

We note that N_e and \tilde{N}_e increase with the temperatures T_{ν_e} and T_{ν_x} . The increase for each N_e follows the increase of the different σ_e . The contribution of the neutrino flux, $\mathcal{F}_{\nu_e}^0$, in N_e is strongly concentrated in the region below 60 MeV. This is because: (i) the mean neutrino energy $\langle E_{\nu_e} \rangle$ of the flux varies from 10.1 to 17.6 MeV approximately [38]; and (ii) the contribution of the product of σ_e with the flux tail is not important. Notice that the ordering of the N_e in Figure 3 is the same as the ordering of σ_e shown in Figure 1. For example, the crossing between N_e ’s of our QRPA and Hybrid model at $T_{\nu_e} \sim 4.8$ MeV originates from the crossing of the corresponding σ_e at $E_\nu \sim 32$ MeV as Figure 1 shows.

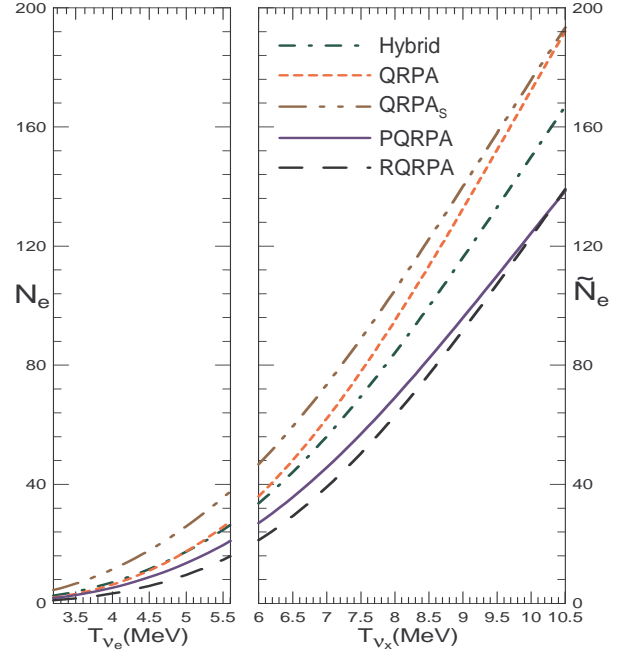


FIG. 3: (Color online) Number of events obtained from the convolution of the neutrino fluxes with the cross section obtained with different nuclear structure models: Hybrid (dashed-dot line) [28], QRPA (dashed line), QRPA_s (dashed-dot-dot line) [18], PQRPA (solid line), and RQRPA (dashed line) [20].

The above behavior also applies to \tilde{N}_e , but they are shifted according to the shift that $\mathcal{F}_{\nu_x}^0$ has with respect to $\mathcal{F}_{\nu_e}^0$. This means that the main contribution to \tilde{N}_e comes from the convolution of $\mathcal{F}_{\nu_x}^0$ with σ_e in the energy interval [18.9, 33.1] MeV where the larger energy flux of ν_x is concentrated. The right panel of Figure 3 shows additional crossings at $T_{\nu_x} \sim 10.5$ MeV which is a result of the corresponding crossings of $\sigma_e(\text{QRPA-QRPA}_s)$ at $E_\nu \sim 56$ MeV and $\sigma_e(\text{PQRPA-RQRPA})$ at $E_\nu \sim 60$ MeV, shown in Figure 1. We conclude that the relevant energy interval for the ν_e - ^{56}Fe reaction is $E_\nu \leq 60$ MeV for the astrophysical parameters adopted in LVD.

In summary, we have employed the projected QRPA to calculate the $^{56}\text{Fe}(\nu_e, e^-)^{56}\text{Co}$ cross section. The calculated cross section is compared with a QRPA calculation with the same interaction showing that the projection procedure is important for medium mass nuclei. The cross section is also compared with other RPA and Hybrid models. The PQRPA yields smaller cross section than almost all RPA models with exception of relativistic QRPA [20] for $E_\nu \leq 60$ MeV. Above this energy and up to $E_\nu = 100$ MeV, the PQRPA leads to the smallest cross section. Therefore, we feel that a more detailed study of allowed and forbidden transitions in the region below $E_\nu = 100$ MeV is imperative, both experimentally and theoretically. In particular, the region with $E_\nu \leq 60$ MeV is the most important for the LVD detector [13].

In a future work we plan to include the MSW effect in the same way as was done by Agafonova *et al.* and an explicit account of the uncertainties in the supernova neutrino flux will be considered.

This work was partially supported by the U.S. DOE grants DE-FG02-08ER41533 and DE-FC02-07ER41457 (UNEDF, SciDAC-2).

-
- [1] H. Duan, G.M. Fuller, J. Carlson, and Y-Z Qian, Phys. Rev. D **74**, 105014 (2006).
 - [2] A. Samana, F. Krmpotić, A. Mariano and R. Zukanovich Funchal, Phys. Lett. **B642**, 100 (2006).
 - [3] LSND Collaboration, C. Athanassopoulos *et al.*, Phys. Rev. C **58**, 2489 (1998); Phys. Rev. Lett. **81**, 1774 (1998).
 - [4] A. C. Hayes and I. S. Towner, Phys. Rev. C **61**, 044603 (2000).
 - [5] C. Volpe, N. Auerbach, G. Colò, T. Suzuki, N. Van Giai, Phys. Rev. C **62**, 015501 (2000).
 - [6] S. Cohen and D. Kurath, Nucl. Phys. **73**, 1 (1965).
 - [7] F. Krmpotić, A. Mariano and A. Samana, Phys. Rev. C **71**, 044319 (2005).
 - [8] KARMEN Collaboration, R. Maschuw *et al.*, Prog. Part. Phys. **40**, (1998) 183; and references therein mentioned.
 - [9] KARMEN Collaboration, R. Maschuw, <http://www-ik1.fzk.de/karmen/cc-e.html/article>
 - [10] S.E. Woosley, D. Hartmann, R.D. Hoffman and W.C. Haxton, Astrophys. J. **356**, 272 (1990).
 - [11] MINOS Collaboration, P. Adamson *et al.*, Phys. Rev. D **76**, 072005 (2007).
 - [12] Y. Efremenko, Nucl. Phys. **B138**(Proc. Suppl), 343 (2005); F.T. Avignone III and Y.V. Efremenko, J. Phys. G **29**, 2615 (2003).
 - [13] N.Yu. Agafonova *et al.*, Astron. Phys. **27**, 254 (2007).
 - [14] F. Krmpotić, A. Mariano and A. Samana, Phys. Lett. **B541**, 298 (2002).
 - [15] F. Krmpotić, A. Mariano, T.T.S. Kuo, and K. Nakayama, Phys. Lett. **B319**, 393 (1993).
 - [16] E.V. Bugaev, G.S. Bisnovatyi-Kogan, M.A. Rudzsky, and Z.F. Seidov, Nucl. Phys. **A324**, 350 (1979).
 - [17] E. Kolbe, K. Langanke and G. Martínez-Pinedo, Phys. Rev. C **60**, 052801 (1999).
 - [18] R. Lazauskas and C. Volpe, Nucl. Phys. **A792**, 219 (2007).
 - [19] C. Volpe, J. Phys. G **30**, L1-L6 (2004).
 - [20] N. Paar, D. Vretenar, T. Marketin and P. Ring, Phys. Rev. C **77**, 024608 (2008).
 - [21] N. Itoh and Y. Kohyama, Nucl. Phys. **A306**, 527 (1978).
 - [22] J. Hirsch and F. Krmpotić, Phys. Rev. C **41**, 792 (1990).
 - [23] J. Hirsch and F. Krmpotić, Phys. Lett. **B246**, 5 (1990).
 - [24] F. Krmpotić, J. Hirsch and H. Dias, Nucl. Phys. **A542**, 85 (1992).
 - [25] F. Krmpotić and Shelly Sharma, Nucl. Phys. **A572**, 329 (1994).
 - [26] J. Hirsch and F. Krmpotić, Phys. Rev. C **41**, 792 (1990).
 - [27] A. Bohr B. R. Mottelson, *Nuclear Structure Vol.I W.A. Benjamin Inc., New York, Amsterdam*, (1969).
 - [28] E. Kolbe and K. Langanke, Phys. Rev. C **63**, 025802 (2001).
 - [29] J. Rappaport *et al.*, Nucl. Phys. **A410**, 371 (1983).
 - [30] P. Sarriuren, E. Moya de Guerra and R. Álvarez-Rodríguez, Nucl. Phys. **A716**, 230 (2003).
 - [31] S. Mintz, J. Phys. G **28**, 451 (2002).
 - [32] M.S. Athar, A. Ahmad and S.K. Singh, Nucl. Phys. **A764**, 551 (2006).
 - [33] E.Kh. Akhmedov, Lectures given at Trieste Summer School in Particle Physics, June 7-9, 1999; arXiv:hep-ph/0001264v2.
 - [34] H. Duan, G. M. Fuller, J. Carlson, and Y-Z. Qian, Phys. Rev. Lett. **99**, 241802 (2007).
 - [35] G.L. Fogli, E. Lisi, A. Mirizzi and D. Montanino, J. Cosmol. Astropart. Phys. **04**, 002 (2005).
 - [36] M.Th. Keil, G.G. Raffelt and H-T. Janka, Astrophys. Jour. **590**, 971 (2003).
 - [37] The importance of configuration mixing in ^{12}C is known since the very first work in p -shell nuclei by Cohen and Kurath in '65 [6].
 - [38] The mean neutrino energy results $\langle E_{\nu_e} \rangle \approx 3.15 T_{\nu_e}$ with the pinching parameter $\eta = 0$.